



Science Arena Publications
Specialty Journal of Engineering and Applied Science

ISSN: 2520-5943

Available online at www.sciarena.com

2019, Vol, 4 (2): 91-113

Exergy Analysis of Waste Heat Recovery in the LNG-Based Combined Cooling and Power (CCP) System and Its Use in GAX Cycles

Peyman Asemani Kalejahi

MA, Department of Mechanical Engineering, Mechanical Engineering Faculty, University of Tabriz, Iran.

Abstract: An LNG-based combined cooling and power (CCP) system and the energy recovery from the waste heat were proposed to be used in a GAX cycle and cooling generation. Modeling the cycle was carried out in EES Software. In order to ensure the precision of the obtained results of the simulation, the LNG-based power generation system and the GAX cycle, was validated by comparing them with the results of the technical literature. The intended combined cycle was reviewed from the first and second laws of thermodynamics` perspective. Furthermore, the capacity of the refrigeration cycle, net generated power of the cycle, energy efficiency, exergy efficiency, and total exergy destruction, as well as the exergy destruction of each component of the cycle have been evaluated. The exergy analysis results showed the great amount of exergy destructs in the combustion chamber and heat exchanger number two, respectively. Also, it was concluded that the use of the GAX refrigeration cycle and energy recovery from the waste heat of the mentioned cycle have been very effective to enhance the overall efficiency of the cycle.

Keywords: Exergy Analysis, Waste Heat Energy, LNG, GAX Cycle.

INTRODUCTION

In most industries, a great amount of thermal energy is generated by the combustion of fossil fuels to generate steam and heat for various uses. Anyhow, we face a significant amount of generated heat as a waste heat that is entered into the environment, and we can use an absorption refrigeration cycle to produce cooling by the lost heat. Environmental issues could be reduced using this energy and converting it into cooling. Considering the provided reasons, it seems that absorption systems have many advantages in comparison to compression systems. However, compression systems still have the major part of the market. In order to enhance the applying of absorption systems, improving efficiency and reducing the prices of these systems must be considered in future studies. Although, different methods have been developed to improve the absorption refrigeration cycles in recent years, such as the two effect absorption refrigeration and the GAX cycles. The energy contained in the absorber is transmitted by the working fluid to the generator in the GAX cycle, thus, some of the thermal energy of the cycle is supplied by the cycle itself, and the thermal energy required by the cycle and the input to the generator decreases through the external low-temperature thermal source and cycle efficiency increases.

On the other hand, by the year 2020, electricity demand is expected to increase by 1% and by 3% for developing countries and industrialized countries respectively (Tsatsaronis and Morosuk, 2010; International energy outlook, 2004). Natural gas (NG) has the utmost importance as an energy source in the 10th century

AD, while LNG technology has been considered by researchers since 1692. In particular, over the past 20 years, due to improvements in liquefaction processes, the LNG technology cost has dropped by 32%. Liquefied Natural Gas (LNG) plays a major role in the globalization and extension of natural gas use (Gas, 2006; Foss, 2003).

A great amount of energy is used to produce LNG at a low temperature (approximately -160°C), which is, in fact, a huge source of refrigeration energy and exergy (Sugiyama et al., 1998). Therefore, the effective use of cooling energy released by LNG evaporation is very important. Greipentrog et al. conducted the integration of a closed gas cycle with LNG energy recovery for the first time (Greipentrog and Sackarendt, 1976). Chiesa described four power plants using LNG energy recovery (Chiesa, 1997). Desideri et al. (2000) presented a cycle that, LNG was utilized to chill the steam turbine output as well as the heat recovery of the HRSG. Hanawa (2000) suggested an Ericsson closed cycle to recover LNG energy.

Some researchers (Karellas, 2013; Shi and Che, 2009) have proposed and developed water- and ammonia – based power generation systems using LNG as a thermal sink. John Szargut et al. (2009) studied combined production system based on energy recovery from LNG. Liu et al. (2009) examined the CCP system with zero pollution based on LNG gasification from the second law of thermodynamics and economic perspective. In another study, Xue et al. (2015), examined the two-stage Organic Rankin Cycle (ORC), (Rankine cycle which its working fluid is organic matter), from the perspective of the first and second laws of thermodynamics in order to gasify the LNG and recover the released energy.

On the other hand, the recovery of refrigeration exergy in the LNG gasification process, that can be carried out by coupling this process with power generation cycles in various ways, has attracted the consideration of many researchers (Karashima and Akutsu, 1982; Velautham, Ito and Takata, 2001). In some of these studies, power generation cycles is Brighton cycle and in some cases, the Rankin cycle or a combination of these two types of cycles is used to generate power.

Wang et al. (2014) suggested a dual cycle using geothermal energy for electricity generation. Besides, they used natural gas as a heat sink. Sun et al. (2012) developed a supercritical cycle for hydrogen production. Likewise, they used natural gas to condense carbon dioxide. Several studies have been conducted over years in a field of power generation systems in which carbon dioxide and LNG have been used as a working fluid to reduce condensation temperature respectively (Song et al., 2012; Emmanuel, Nicolas and Martin, 2009).

Furthermore, several studies have been conducted on GAX absorption refrigeration cycles in recent years, including Ramesh Kumar et al. (2008). Altenkirch (1913) proposed ideal GAX cycle in 1611. Garimella et al. (1996), reviewed the GAX heat pump cycle for the use of heating and cooling and examined the effect of ambient temperature on the performance of the cycle, and reported that the ambient temperature of 8 and 32 degrees Celsius, the cycle efficiency for heating and cooling is 1.12 and 2.602, respectively. Ng et al. (1998), studied GAX 2 TR gas-fired cycle experimentally and reported that the cycle efficiency is 2.8 in a condition that each component including generator, condenser, evaporator, and absorber are at 220, 44, 2, and 41 degree of Celsius, respectively. In the present research, a thermodynamic cycle of co-generation for the purpose of electricity generation and gasification of LNG has been simulated using the EES software and analyzed from the perspective of the first and second laws of thermodynamics. It is worth noting that the waste heat of the upstream cycle has been recovered and used to run the GAX refrigeration cycle.

Methods and Material

Figure 1 shows the schematic view of the combined cycle of an LNG-based co-generation and its waste heat recovery in the GAX cycle. As shown in Fig. 1, the upstream cycle consisted of two Brighton cycles that were related in a cascade order. In the upstream cycle, at first the air was compressed via compressor and then entered the middle chiller to increase its density and, as a result, reduced the consumed work in the cycle. Afterward, it was entered into the second compressor and the pressure raised to the combustion chamber pressure level. In the combustion chamber, methane reacted with air as fuel and accordingly, combustion took

place. Hot gases were exhausted from the combustion chamber then entered the turbine, and consequently generated power. The heat wasted by the relatively hot gases out of the turbine of the upstream cycle entered the the heat exchanger and acted as a hot source for the Brighton downstream cycle. N₂ acted as a working fluid in the downstream cycle that after compressing in the compressor, it entered the heat exchanger and then entered the turbine and generated the desired power of the cycle. The output N₂ from the turbine was entered into a heat exchanger and acted as a heat source for a designed LNG gasification cycle. Finally, the Brighton upstream cycle used the thermal energy released from the GAX compressor middle chiller output to run the GAX cycle.

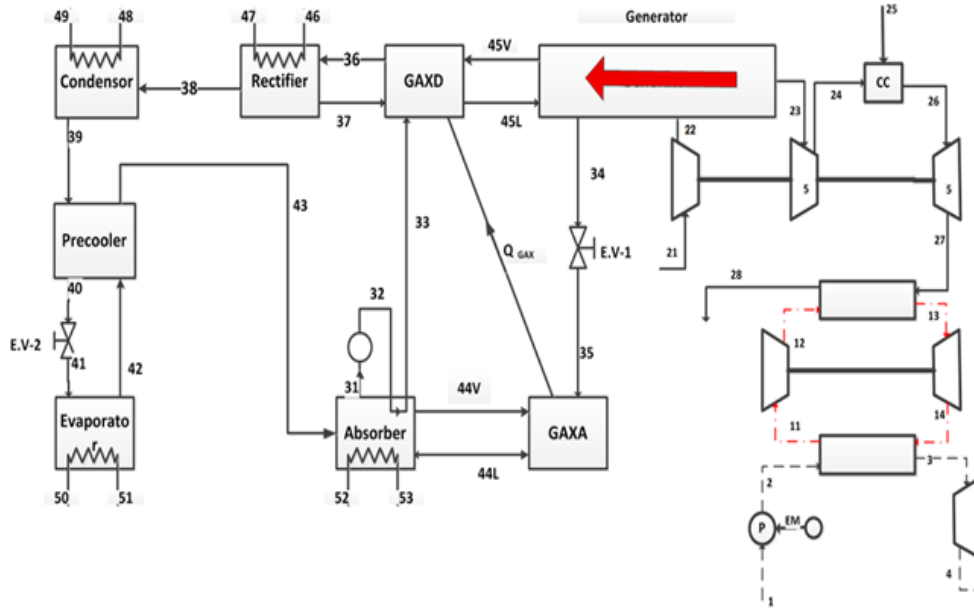


Figure 1. Schematics of co-generation cycle based on LNG and GAX cycle

Energy analysis of the combined cycle of co-generation based on LNG and GAX cycle

Having neglected the kinetic and potential energy of the fluid in the input and output of the control volume, the first law of thermodynamics has been defined as follows:

$$\dot{Q} - \dot{W} = \sum_i \dot{m}_i h_i - \sum_e \dot{m}_e h_e \tag{1}$$

Which \dot{Q} and \dot{W} represent the input and output thermal energy of control volume, respectively. Also, \dot{m} and h represent mass flow and specific enthalpy of the flow, respectively.

Table 1. The governing thermodynamic equation based on the conservation of energy for different components of the LNG-based co-generation GAX cycl

Components	Energy relations	Auxiliary equations
Generator	$\dot{Q}_{gen,tot} = \dot{m}_{36}h_{36} + \dot{m}_{34}h_{34} - \dot{m}_{33}h_{33} - \dot{m}_{37}h_{37}$	-
GAXD	$\dot{Q}_{rq} = \dot{m}_{36}h_{36} + \dot{m}_{45L}h_{45L} - \dot{m}_{33}h_{33} - \dot{m}_{37}h_{37} - \dot{m}_{45V}h_{45V}$	-
GAXA	$\dot{Q}_{av} = \dot{m}_{44L}h_{44L} - \dot{m}_{44V}h_{44V} - \dot{m}_{35}h_{35}$	-
Absorber	$\dot{Q}_{abs,tot} = \dot{m}_{33}h_{33} + \dot{m}_{31}h_{31} - \dot{m}_{43}h_{43} - \dot{m}_{35}h_{35} - \dot{m}_{32}h_{32}$	-
Evaporator	$\dot{Q}_{eva} = \dot{m}_{41}(h_{42} - h_{41})$	-
Condenser	$\dot{Q}_{cond} = \dot{m}_{39}(h_{39} - h_{38})$	-

Rectifier	$\dot{Q}_{rec} = \dot{m}_{37}h_{37} + \dot{m}_{38}h_{38} - \dot{m}_{36}h_{36}$	-
Pump 1	$\dot{W}_{P1} = \dot{m}_{31}(h_{37} - h_{32})$	$\eta_p = \frac{\dot{W}_{s,p}}{\dot{W}_p}$
Expansion Valve 1	$0 = (h_{34} - h_{35})$	-
Expansion Valve 2	$0 = (h_{40} - h_{41})$	-
Pre- Cooler	$0 = (h_{43} - h_{40}) - (h_{42} - h_{39})$	$\varepsilon = \frac{C_{cool}\Delta T}{C_{min}\Delta T_{max}}$
Compressor 1	$\dot{W}_{c1} = \dot{m}_{air}(h_{21} - h_{22})$	$\eta_{comp} = \frac{\dot{W}_{s,t}}{\dot{W}_{a,t}},$ $\dot{m}_{air} = \dot{n}_{air} \cdot M_{air}$
Compressor 2	$\dot{W}_{c2} = \dot{m}_{air}(h_{24} - h_{23})$	$\eta_{comp} = \frac{\dot{W}_{s,t}}{\dot{W}_{a,t}}$
Compressor 3	$\dot{W}_{c3} = \dot{m}_{N2}(h_{12} - h_{13})$	$\eta_{comp} = \frac{\dot{W}_{s,t}}{\dot{W}_{a,t}}$
Turbine 1	$\dot{W}_{t1} = \dot{m}_p(h_{26} - h_{27})$	$\dot{m}_p = \dot{m}_{fuel} + \dot{m}_{air},$ $\eta_{turb} = \frac{\dot{W}_{a,t}}{\dot{W}_{s,t}}$
Turbine 2	$\dot{W}_{t2} = \dot{m}_{N2}(h_{13} - h_{14})$	$\eta_{turb} = \frac{\dot{W}_{a,t}}{\dot{W}_{s,t}}$
Turbine 3	$\dot{W}_{t3} = \dot{m}_{LNG}(h_3 - h_4)$	$\eta_{turb} = \frac{\dot{W}_{a,t}}{\dot{W}_{s,t}}$
Heat exchanger 1	$\dot{m}_{N2}(h_{13} - h_{12}) = \dot{m}_p(h_{27} - h_{28})$	$\eta_{HX2} = \frac{h_{13} - h_{12}}{h_{13} - h_{27}}$
Heat exchanger 2	$\dot{m}_{N2}(h_{14} - h_{12}) = \dot{m}_{LNG}(h_3 - h_2)$	$\eta_{HX3} = \frac{h_3 - h_2}{h_3 - h_{14}}$
Pump 2	$\dot{W}_{p2} = \dot{m}_{LNG}(h_2 - h_1)$	$\eta_p = \frac{\dot{W}_{s,p}}{\dot{W}_p}$
Combustion chamber	$-0.02 \cdot \lambda \cdot LHV_{CH4} = (1 + \lambda)h_{26} - h_{24} - \lambda h_{25}$	$\lambda = \frac{\dot{n}_{fuel}}{\dot{n}_{air}}, \dot{n}_{fuel} = \frac{\dot{m}_{fuel}}{M_{fuel}},$ $\dot{n}_{air} = \frac{\dot{m}_{air}}{M_{air}}$

Exergy analysis of the combined cycle of co-generation based on LNG and GAX cycle

In technical literature, the sum of physical, kinetic and potential exergy is known as thermomechanical exergy. Therefore, the exergy of a thermodynamic system can be divided into two distinct parts: thermomechanical and chemical exergy. The present study aimed to obtain both thermomechanical and chemical exergy for fluids at different points in the cycle due to the importance of chemical exergy in calculating the unit cost of fuel and products of the thermodynamic cycle components.

The relation of thermomechanical exergy can be presented as follows:

$$\dot{E}^{th} = (h_i - h_0) + T_0(s_i - s_0) \quad (2)$$

The present work considers the chemical exergy of the exhaust gas from the engine as diffusive exergy, which only includes gases that exist both in the system and ambient. In the present study, these mentioned gases included N₂, CO₂, O₂ and H₂O. For this case, it was essential to determine the temperature and pressure of the actual dead state (ambient). In the present work, the ambient temperature and pressure was T₀ = 298k P₀ = 1bar, respectively. Furthermore, the share of a mixture of these gases in the ambient state has been presented according to the Table (2).

Table 2. Mixture of gases in ambient condition

component	By volume %			
	N2	O2	H2O	CO2
	77.48	20.59	1.9	0.03

The chemical exergy can be obtained via the following equation:

$$E_i^{CH} = -\bar{R}T_0 \sum y_k \ln \frac{y_{0,k}}{y_k} \quad (3)$$

Where y_k and $y_{0,k}$ are the molar fracture of limited and actual dead state, respectively.

Exergy destruction can also be obtained for each component of the cycle by the following equation:

$$\dot{E}_{D,k} = \dot{E}_{F,k} - \dot{E}_{P,k} - \dot{E}_{L,k} \quad (4)$$

Table 3. Exergy balance according to the second law of thermodynamic for each component of LNG-based combined co-generation and GAX cycles

Components	Exergy balance
Generator	$\dot{I}_{des\&abs} = T_0(\dot{m}_{34}S_{34} + \dot{m}_{36}S_{36} + \dot{m}_{35}S_{35} - \dot{m}_{34}S_{34} - \dot{m}_{37}S_{37} - \dot{m}_{43}S_{43} - \dot{m}_{32}S_{32} + \dot{m}_g(s_{out,gen} - s_{in,gen}) + \dot{m}_{abs}(s_{out,abs} - s_{in,abs}))$
GAXD	$\dot{I}_{des\&abs} = T_0(\dot{m}_{34}S_{34} + \dot{m}_{36}S_{36} + \dot{m}_{35}S_{35} - \dot{m}_{34}S_{34} - \dot{m}_{37}S_{37} - \dot{m}_{43}S_{43} - \dot{m}_{32}S_{32} + \dot{m}_g(s_{out,gen} - s_{in,gen}) + \dot{m}_{abs}(s_{out,abs} - s_{in,abs}))$
GAXA	$\dot{I}_{des\&abs} = T_0(\dot{m}_{34}S_{34} + \dot{m}_{36}S_{36} + \dot{m}_{35}S_{35} - \dot{m}_{34}S_{34} - \dot{m}_{37}S_{37} - \dot{m}_{43}S_{43} - \dot{m}_{32}S_{32} + \dot{m}_g(s_{out,gen} - s_{in,gen}) + \dot{m}_{abs}(s_{out,abs} - s_{in,abs}))$
Absorber	$\dot{I}_{des\&abs} = T_0(\dot{m}_{34}S_{34} + \dot{m}_{36}S_{36} + \dot{m}_{35}S_{35} - \dot{m}_{34}S_{34} - \dot{m}_{37}S_{37} - \dot{m}_{43}S_{43} - \dot{m}_{32}S_{32} + \dot{m}_g(s_{out,gen} - s_{in,gen}) + \dot{m}_{abs}(s_{out,abs} - s_{in,abs}))$
Evaporator	$\dot{I}_{eva} = T_0(\dot{m}_{42}S_{42} - \dot{m}_{41}S_{41} + \dot{m}_e(s_{out,eva} - s_{in,eva}))$
Condenser	$\dot{I}_{cond} = T_0(\dot{m}_{39}S_{39} - \dot{m}_{38}S_{38} + \dot{m}_{cond}(s_{out,cond} - s_{in,cond}))$
Rectifier	$\dot{I}_{rec} = T_0(\dot{m}_{37}S_{37} + \dot{m}_{38}S_{38} - \dot{m}_{36}S_{36} + \dot{m}_{rec}(s_{out,rec} - s_{in,rec}))$
Pump 1	$\dot{I}_p = T_0(\dot{m}_{32}S_{32} - \dot{m}_{31}S_{31})$
Expansion Valve 1	$\dot{I}_{EV1} = T_0(\dot{m}_{35}S_{35} - \dot{m}_{34}S_{34})$
Expansion Valve 2	$\dot{I}_{EV2} = T_0(\dot{m}_{40}S_{40} - \dot{m}_{41}S_{41})$
Pre-Cooler	$\dot{I}_{RHX} = T_0(\dot{m}_{40}S_{40} + \dot{m}_{43}S_{43} - \dot{m}_{39}S_{39} - \dot{m}_{42}S_{42})$
Compressor 1	$\dot{E}_{D,comp1} = \dot{E}_{21} + \dot{W}_{comp1} - \dot{E}_{22}$
Compressor 2	$\dot{E}_{D,comp2} = \dot{E}_{23} + \dot{W}_{comp2} - \dot{E}_{24}$
Compressor 3	$\dot{E}_{D,comp3} = \dot{E}_{11} + \dot{W}_{comp3} - \dot{E}_{12}$
Turbine 1	$\dot{E}_{D,turb1} = \dot{E}_{26} + \dot{W}_{turb1} - \dot{E}_{27}$
Turbine 2	$\dot{E}_{D,turb2} = \dot{E}_{13} + \dot{W}_{turb2} - \dot{E}_{14}$
Turbine 3	$\dot{E}_{D,turb3} = \dot{E}_3 + \dot{W}_{turb3} - \dot{E}_4$
Heat exchanger 1	$\dot{E}_{D,HX2} = \dot{E}_{27} + \dot{E}_{12} - \dot{E}_{28} - \dot{E}_{13}$
Heat exchanger 2	$\dot{E}_{D,HX3} = \dot{E}_{14} + \dot{E}_2 - \dot{E}_{11} - \dot{E}_3$
Pump 2	$\dot{E}_{D,pump} = \dot{E}_1 + \dot{W}_{pump} - \dot{E}_2$

Combustion chamber	$\dot{E}_{D,C.C.} = \dot{E}_{24} + \dot{E}_{25} - \dot{E}_{26}$
--------------------	---

The evaluation of the combined cycle from the perspective of the first and second laws of the thermodynamics of equation (5) stated the efficiency of the first law as:

$$\eta = \frac{\dot{Q}_{evap} + \dot{W}_{net}}{\dot{m}_{fuel} \times LHV_{CH4}} \tag{5}$$

Which \dot{m}_{fuel} shows the mass flow of fuel consumption in the cycle and represents the low heat value of the fuel. Furthermore, \dot{Q}_{evap} is the amount of heat absorbed from the chilled fluid in the GAX cycle and \dot{W}_{net} is the net value of the work of the combined cycle and follows the following relationships:

$$\dot{Q}_{eva} = \dot{m}_{41}(h_{42} - h_{41}) \tag{6}$$

$$\dot{W}_{net} = \dot{W}_{turb1} + \dot{W}_{turb2} + \dot{W}_{turb3} - \dot{W}_{comp1} - \dot{W}_{comp2} - \dot{W}_{comp3} - \dot{W}_{pump1} - \dot{W}_{pump2} \tag{7}$$

The second law efficiency has been determined as:

$$\eta_{II} = \frac{\dot{Q}_{eva} \left| 1 - \frac{T_0}{T_b} \right| + \dot{W}_{net}}{\dot{m}_{fuel} \cdot \dot{E}_{ch,fuel} + \dot{E}_1} \tag{8}$$

Which T_b is the chiller temperature in contact with the chiller body and is estimated as $T_{41} + 5$. Likewise, $\dot{E}_{ch,fuel}$ is the chemical exergy of methane that is equal to 51521.75KJ/Kg.

Findings

In the present study, the gas turbine cascade cycle has been combined with GAX refrigeration cycle based on the Liquefied Natural Gas in order to generate power and has been reviewed from the first and second laws of thermodynamics perspective. Primary, power generation cycle based on LNG has been validated as an upstream cycle hand with the results in the technical literature. Then the results of the thermodynamic analysis of the GAX refrigeration cycle have been verified in comparison to the results in the technical literature. Finally, the mentioned combined cycle has been analyzed from the perspective of energy and exergy. Accordingly, the effects of the evaporator temperature, the pressure ratio of the compressor of Brighton cycle with methane fuel, the pressure ratio of the compressor of Brighton cycle with N2 working fluid on the net power of the cycle, the refrigeration capacity, Energy efficiency, and exergy efficiency and exergy destruction in different cycle components have been evaluated.

1. Modeling and validating the obtained results of the analysis of the LNG-based power generation cycle

The performance results of the LNG-based power generation cycle have been evaluated with the results presented by Morosuk et al. (2011). Table 4 represents the obtained results of the present study and Morosuk et al.(2011). These results were well matched so the present modeling was reliable.

Table 4. Comparison of the results of the present study and the study conducted by Morosuk et al.

State point	Material steam	·m(kg/s)	T(C)o		P(bar)		h(kJ/kg)		e(kJ/kg)	
			Morosuk et al	Present study						
1	LNG	65.03	-160	-160	10	10	-904.5	-904.5	1009	1019.6
2	LNG	65.03	-144	-143.8	272	272	-812.4	810.9	1029	1038.46
3	NG	65.03	86	85.12	270	270	-5.4	-9.057	803	811.8
4	NG	65.03	2	2.177	80	80	-150.2	-153.9	631	637.8

11	N2	217	-129	-128.8	2.85	2.85	-162.8	-159.6	147	146.24
12	N2	217	70	69.49	42.75	42.75	41.1	46.19	324	324.85
13	N2	217	415	420.1	40.61	40.61	414.7	419.2	477	478
14	N2	217	101	105.1	3	2.99	79.1	83.25	104	105
21	Air	209	15	15	1.013	1.013	-100.2	-173.56	1	4.0
22	Air	209	242	238.9	6.66	6.66	131.4	56.15	218	212.59
23	Air	209	117	117	6.527	6.53	3.1	-60.89	171	167.6
24	Air	209	416	409.1	42.55	43.47	315.2	237.49	469	450.83
22	CH4	5.1	15	15	45	45	-4689	-4684.5	52100	48140.9
22	combustion gases	214.1	1290	1290	41.06	41.95	123	100.07	1290	1253.33
22	combustion gases	214.1	435	440.1	1.08	1.08	-939.7	-940.86	199	205.94
22	combustion gases	214.1	90	84.49	1.025	1.025	-1318	-1326.67	27	32.4

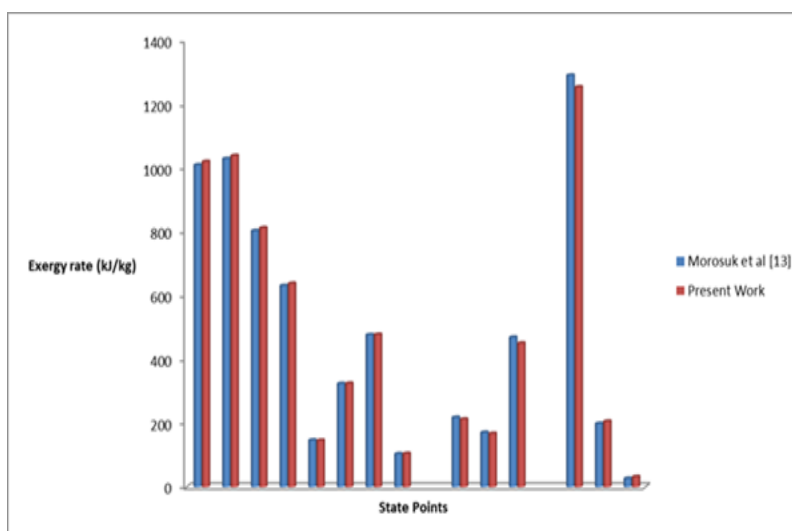


Figure 2. Comparison of each component exergy of the present study to the study conducted by Morosuk et al. (2011)

As shown in the bar graph of Fig. 2, the amount of exergy obtained through the simulation performed in the present study was well consistent with the results of the Morosuk et al. of various components of the cycle. It can be claimed that the second law analysis of the present cycle has been carried out with great precision.

2. Validation of the GAX refrigeration cycle with the models in the technical literature

The results of the performance of the GAX absorption refrigeration cycle have been compared with the results presented by Ramesh Kumar. As shown in Figure 3, the results were consistent. For the validation of the B-model hybrid cycle, the results presented by Kong were used (see Figure 4).

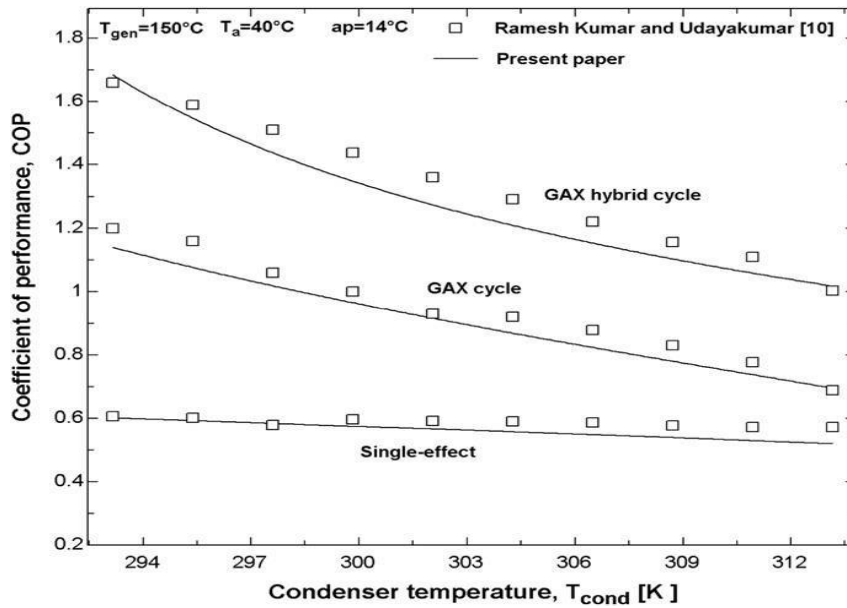


Figure 3. Variation of the first law efficiency with the increase in condenser temperature for single-effect absorption, conventional GAX, Hybrid GAX A-model cycles

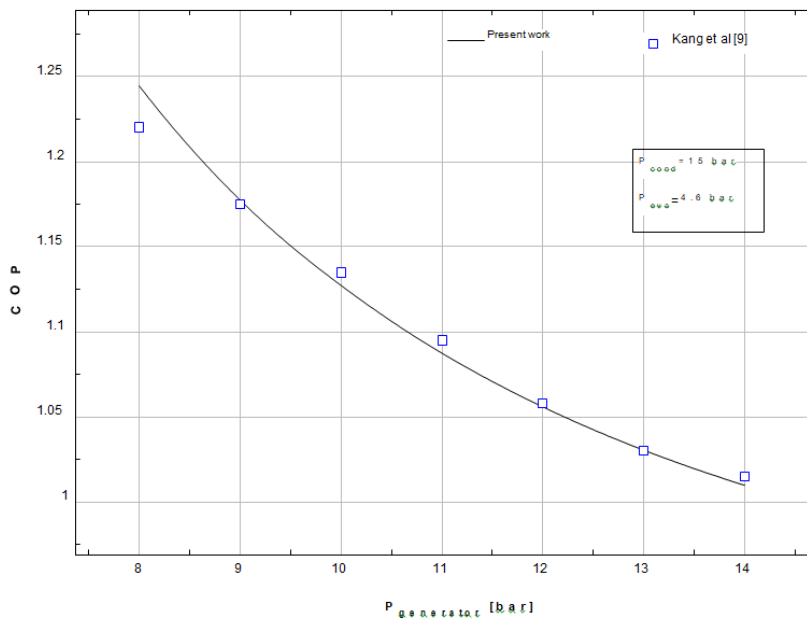


Figure 4. Variation of the first law efficiency with the increase in generator pressure for Hybrid GAX A-model cycle

3. The effects of the functional temperature of the evaporator, generator, No. 1 compressor pressure ratio, and pressure ratio of the Brighton mid-cycle compressor with an N2 working fluid on cycle performance

Figures 5-9, show the effects of evaporator temperatures on refrigeration capacity, power generation, energy efficiency, exergy efficiency, and exergy destruction of the cycle. The pressure ratio of Compressor No. 1 has been assumed to be 6.575 and the pressure ratio in the Brighton cycle with an N2 working fluid was 15.

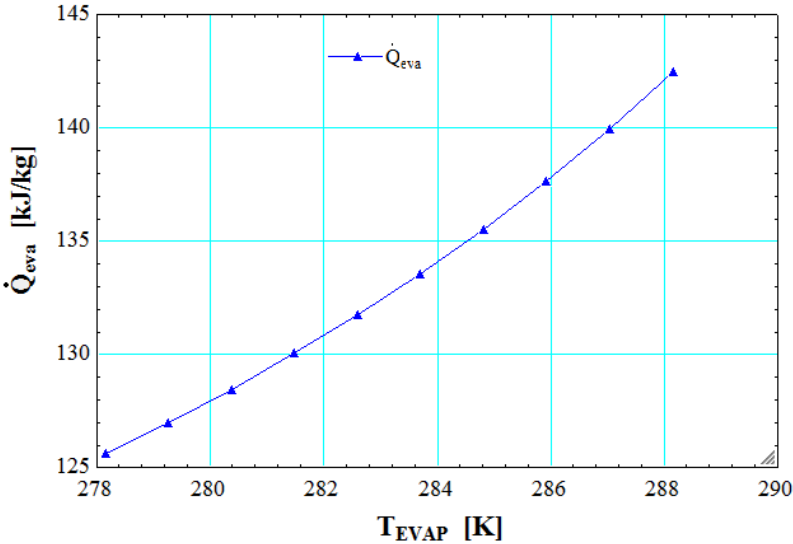


Figure 5. Variation of refrigeration capacity in terms of evaporator temperature

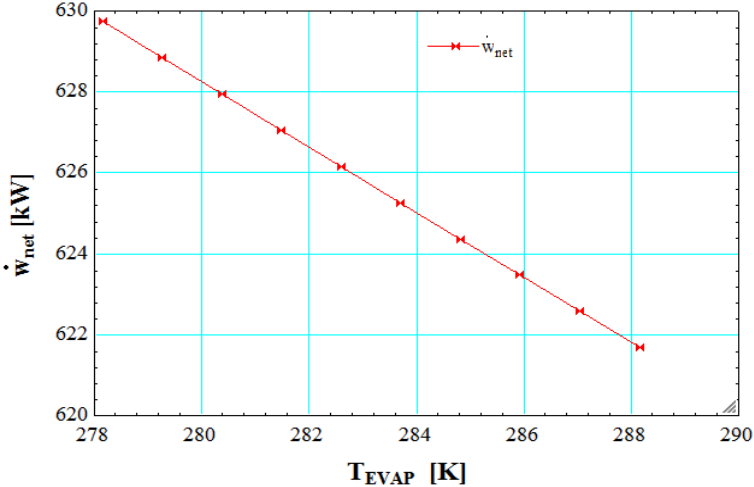


Figure 6. Variation of net power generation in terms of evaporator temperature

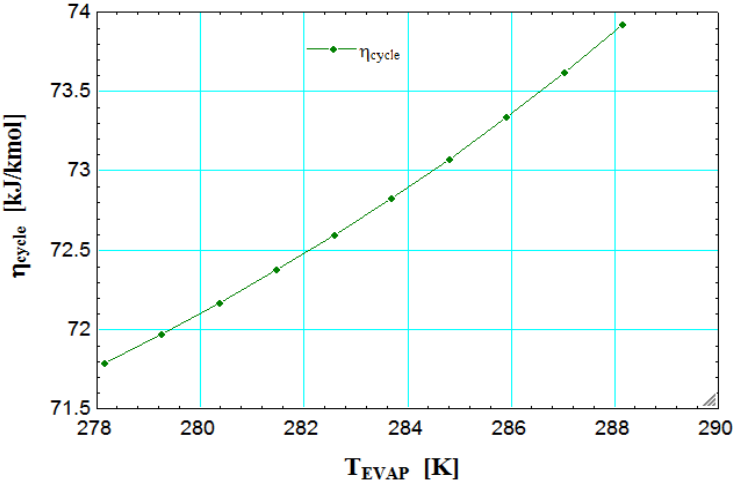


Figure 7. Variation of energy efficiency in terms of evaporator temperature

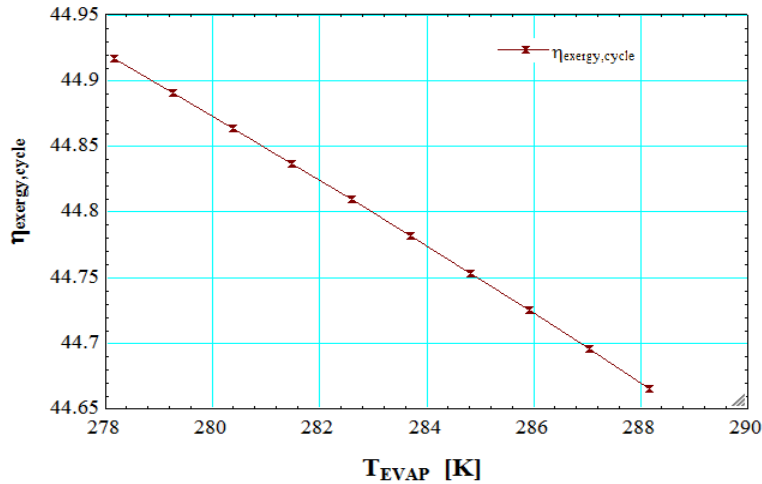


Figure 8. Variation of exergy efficiency in terms of evaporator temperature

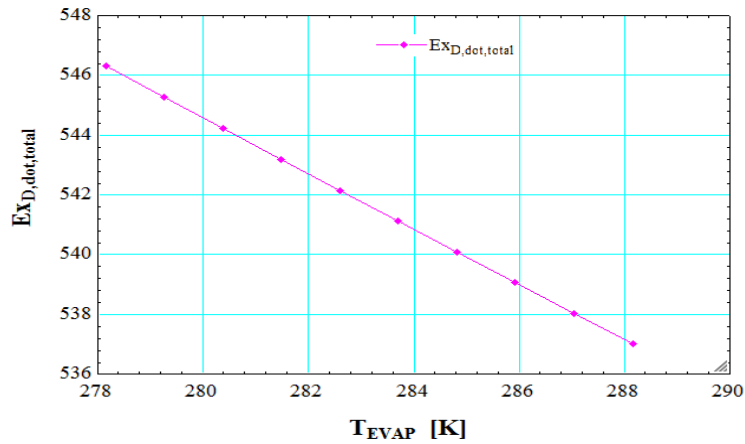


Figure 9. Variation of exergy destruction in terms of evaporator temperature

Figures 10-14, show the effects of pressure ration of compressor No.1 on refrigeration capacity, power generation, energy efficiency, exergy efficiency, and exergy destruction of the cycle. The evaporator temperature was assumed to be 2 degrees Celsius and the pressure ratio in the Brighton cycle with an N2 working fluid was 12.

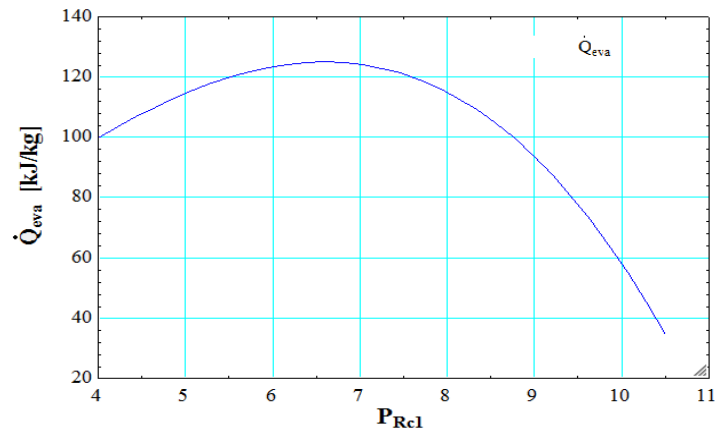


Figure 10. Variation of refrigeration capacity in terms of compressor No.1 pressure ratio

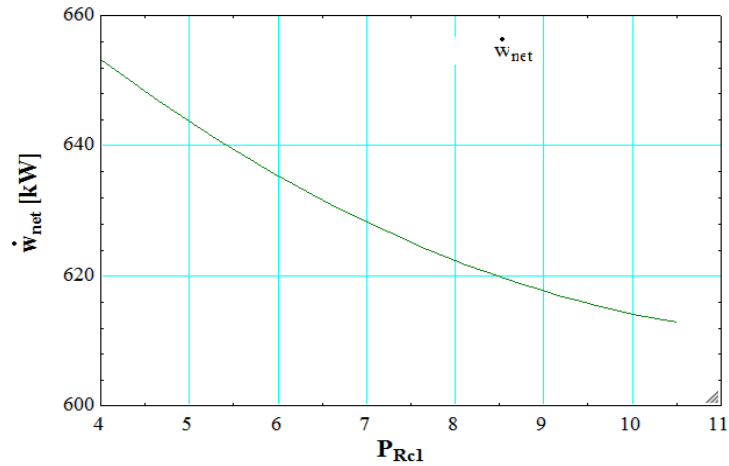


Figure 11. Variation of cycle net power generation in terms of compressor No.1 pressure ratio

According to figure (11), with the increase of the compressor No.1 pressure ratio, the net power of the cycle decreased due to the fact that with the increase in the compressor pressure, the consumption work increases and this caused the net power of the cycle to be reduced.

Given that, the energy efficiency of the cycle was affected by changes in refrigeration capacity and the net power of the cycle. It was expected that the energy efficiency of the cycle increasing in a range and decreasing in another range as the pressure ratio of compressor No.1 would increase. According to the chart, due to these changes, the refrigeration capacity should have an extremum point. Figure 10 illustrates the energy efficiency variation diagram in terms of compressor No.1 pressure ratio.

Figures 13 and 14 illustrate the changes in exergy efficiency and the total exergy destruction of the cycle in terms of the compressor No. 1 pressure ratio.

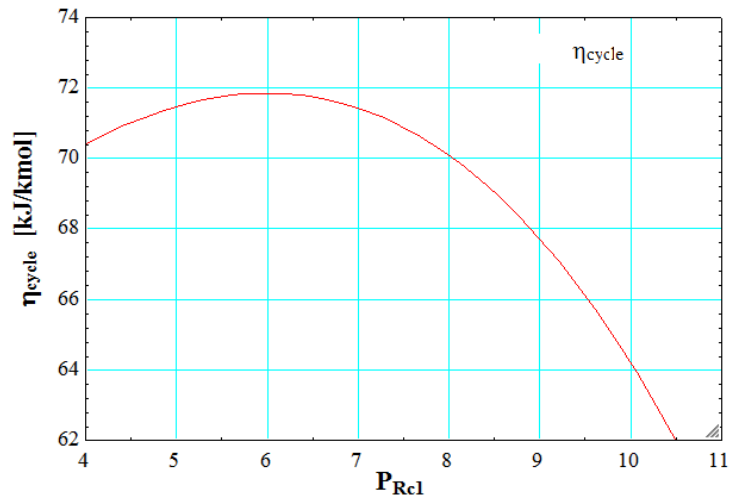


Figure 12. Variation of cycle energy efficiency in terms of compressor No.1 pressure ratio

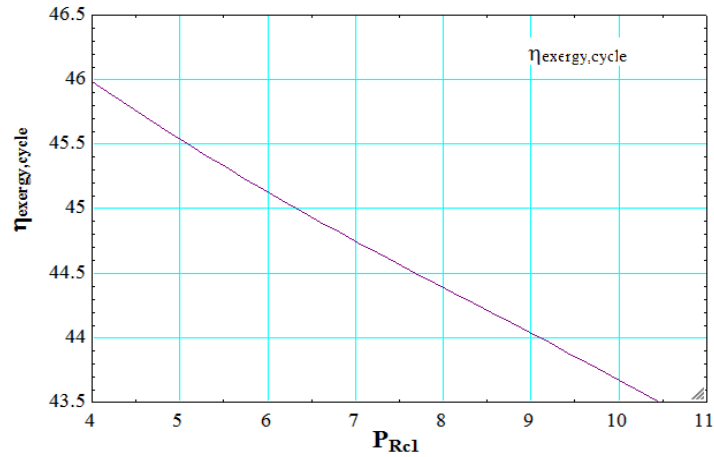


Figure 13. Variation of cycle exergy efficiency in terms of compressor No.1 pressure ratio

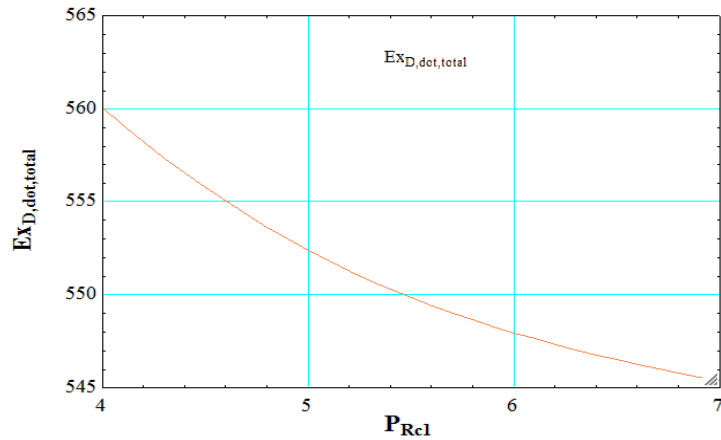


Figure 14. Variation of cycle total exergy destruction in terms of compressor No.1 pressure ratio

Figures 15-19, show the effects of pressure ratio of compressor No.1 on refrigeration capacity, power generation, energy efficiency, exergy efficiency, and exergy destruction of the cycle. The evaporator temperature has been assumed to be 5 degrees Celsius and the pressure ratio in the Brighton cycle with an N2 working fluid was 15.

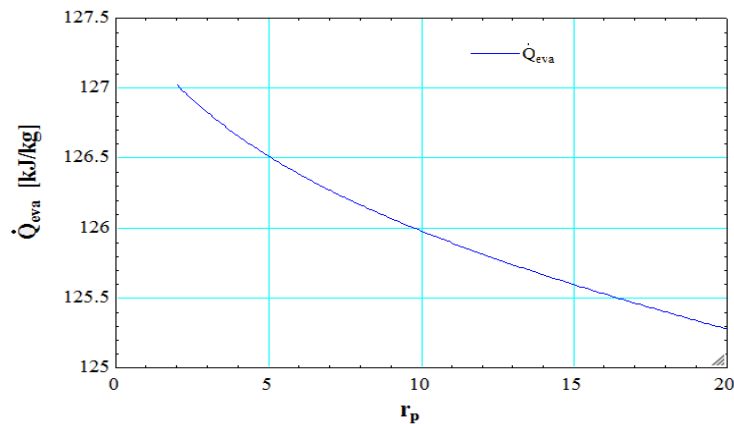


Figure 15. Variation of cycle refrigeration capacity in terms of the pressure ratio in the Brighton cycle with an N2 working fluid

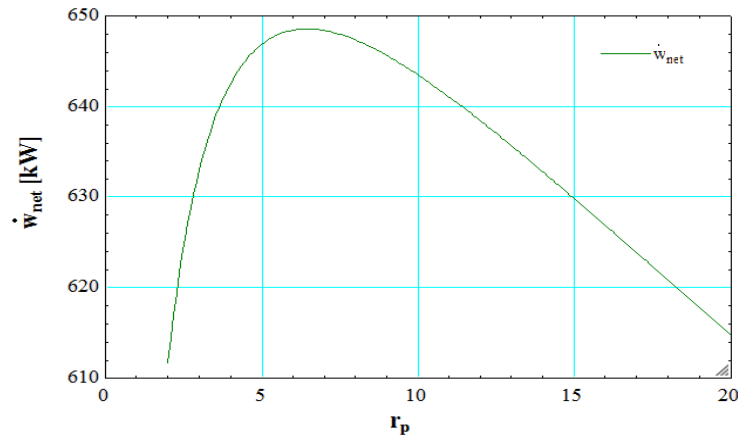


Figure 16. Variation of cycle net power generation in terms of the pressure ratio in the Brighton cycle with an N2 working fluid

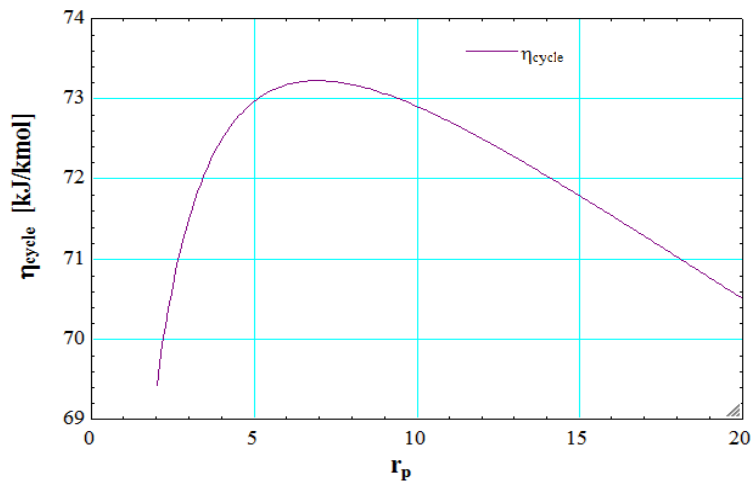


Figure 17. Variation of energy efficiency in terms of the pressure ratio in the Brighton cycle with an N2 working fluid

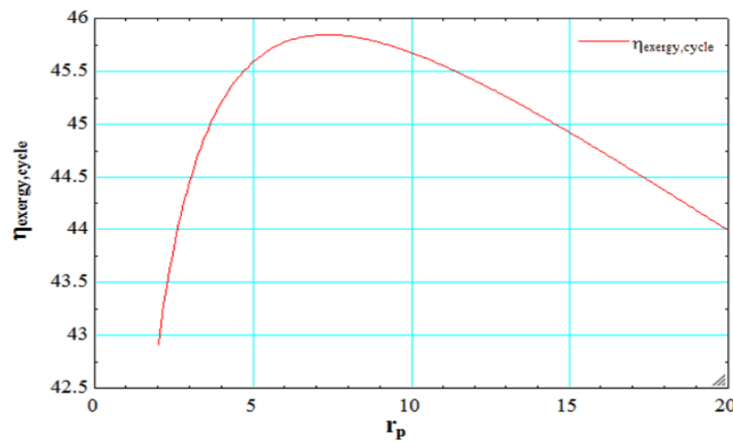


Figure 18. Variation of exergy efficiency in terms of the pressure ratio in the Brighton cycle with an N2 working fluid

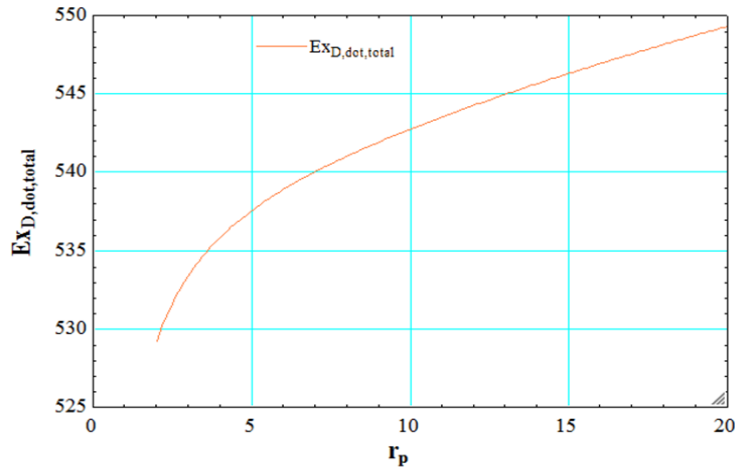


Figure 19. Variation of exergy destruction in terms of the pressure ratio in the Brighton cycle with an N2 working fluid

Figures 20 and 21 show the effect of the generator temperature on the refrigeration capacity and net power generation of the cycle, respectively. It is evident that, as the generator temperature increased, the amount of refrigeration capacity and the net power generation of the cycle decreased, which led to a decrease in cycle energy efficiency as shown in Fig.22.

Furthermore, by increasing the generator temperature, as shown in Fig. 23, unlike the energy efficiency, the exergy efficiency of the combined cycle increased. These results can be justified by the fact that an increase in generator temperature reduces the total exergy destruction of the cycle that is shown in Fig. 24, thus the efficiency of the second law of thermodynamics increased.

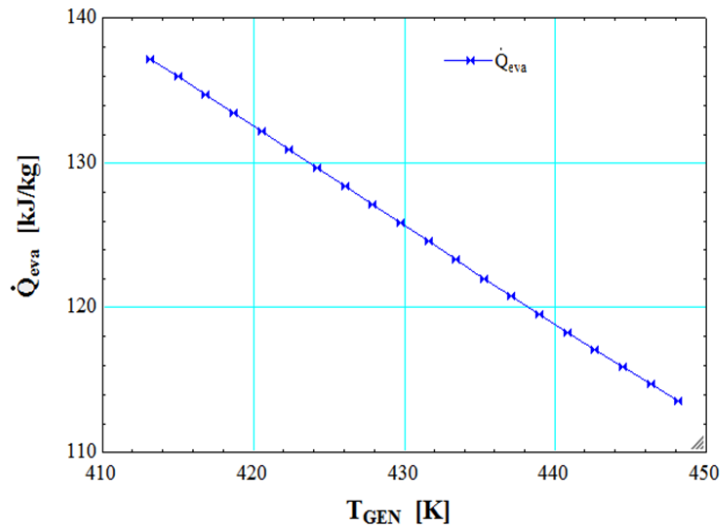


Figure 20. Variation of refrigeration capacity of combined cycle in terms of the generator temperature

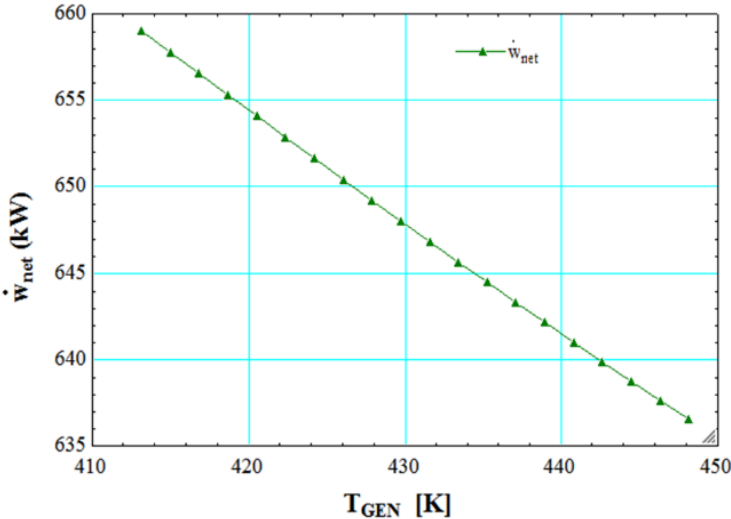


Figure 21. Variation of net power generation of combined cycle in terms of the generator temperature

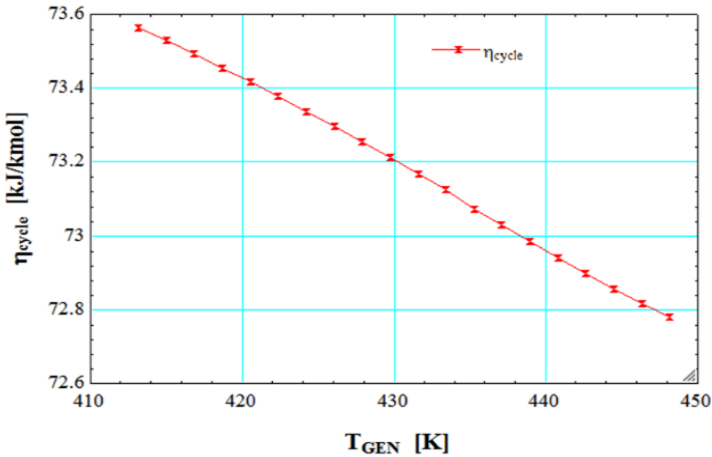


Figure 22. Variation of energy efficiency of combined cycle in terms of the generator temperature

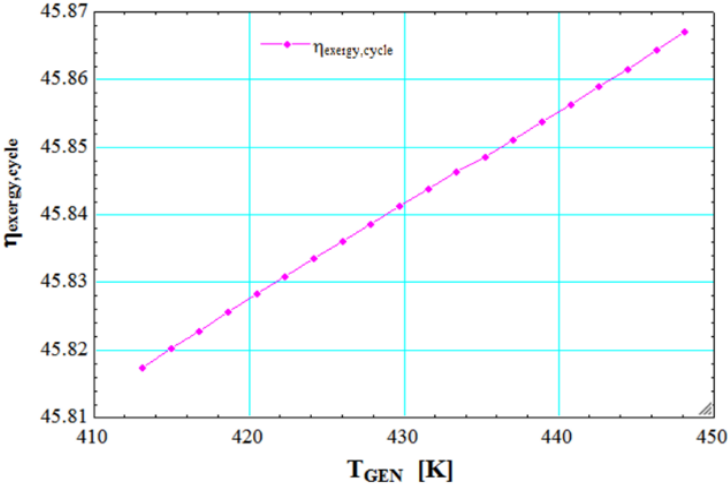


Figure 23. Variation of exergy efficiency of combined cycle in terms of the generator temperature

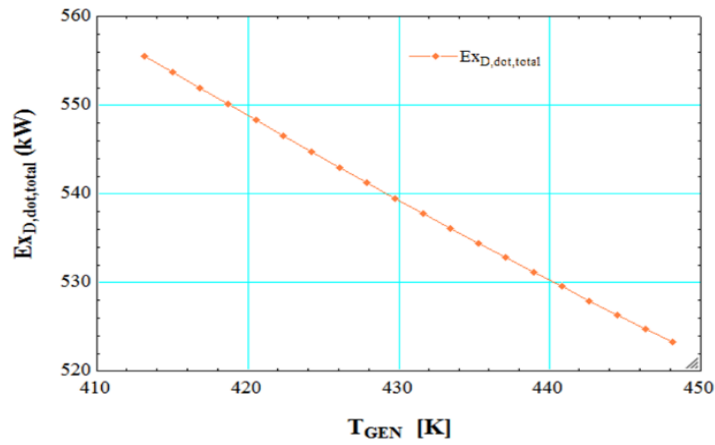


Figure 24. Variation of exergy destruction of combined cycle in terms of the generator temperature

Figures 25-29 illustrate the effect of pressure ratio of points 24 to 21, namely P_{Rt} on the performance of combined cycle.

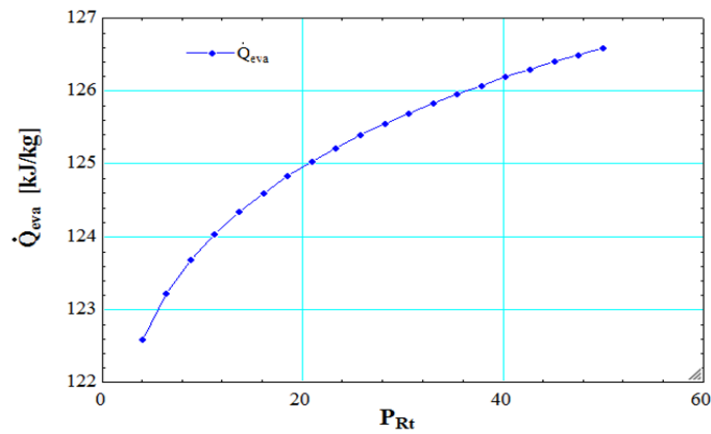


Figure 25. Variation of refrigeration capacity of combined cycle in terms of the pressure ratio between 21 and 24 points

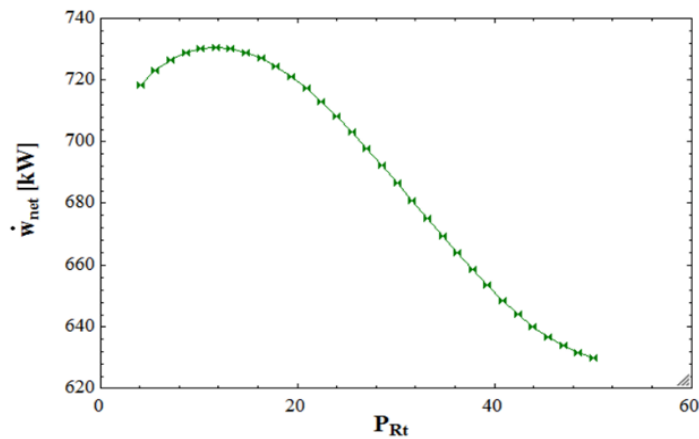


Figure 26. Variation of net power generation of combined cycle in terms of the pressure ratio between 21 and 24 points

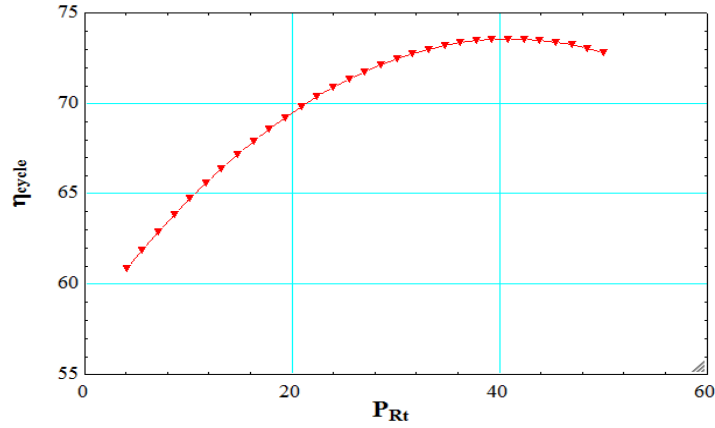


Figure 27. Variation of energy efficiency of combined cycle in terms of the pressure ratio between 21 and 24 points

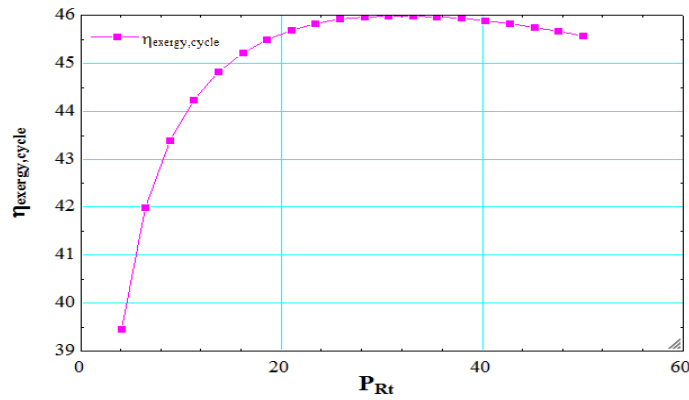


Figure 28. Variation of exergy efficiency of combined cycle in terms of the pressure ratio between 21 and 24 points of combined cycle in terms of the pressure ratio between 21 and 24 points

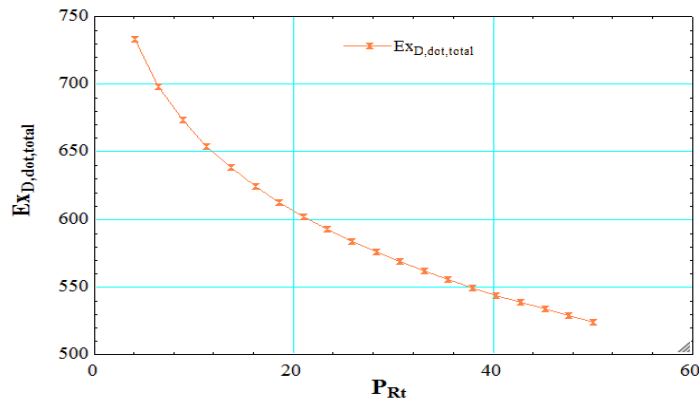


Figure 29. Variation of exergy destruction of combined cycle in terms of the pressure ratio between 21 and 24 points

In order to further elucidate the LNG-based power generation cycle in Figures 30-38, the effect of parameters such as compressor No. 1 pressure ratio, Brighton compressor pressure ratio, and pressure ratio between points 21 and 24 on power generation of the cycle, energy efficiency and exergy efficiency of the cycle have been investigated.

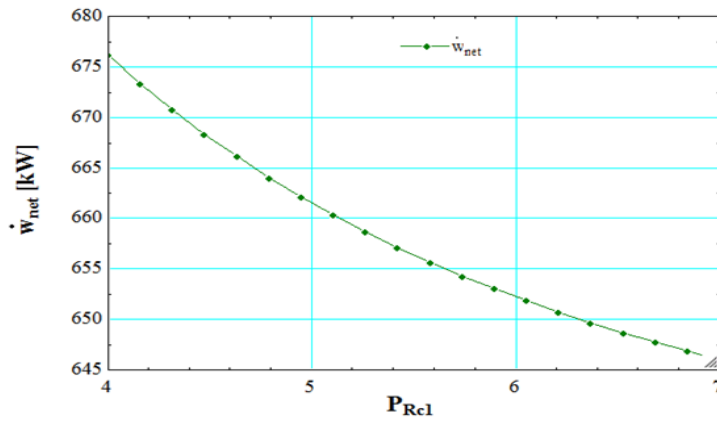


Figure 30. Variation of net power generation of LNG-based cycle in terms of the compressor No.1 pressure ratio

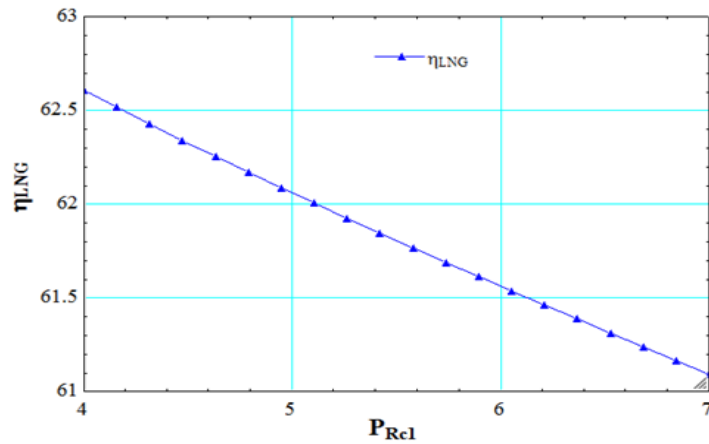


Figure 31. Variation of energy efficiency of LNG-based cycle in terms of the compressor No.1 pressure ratio

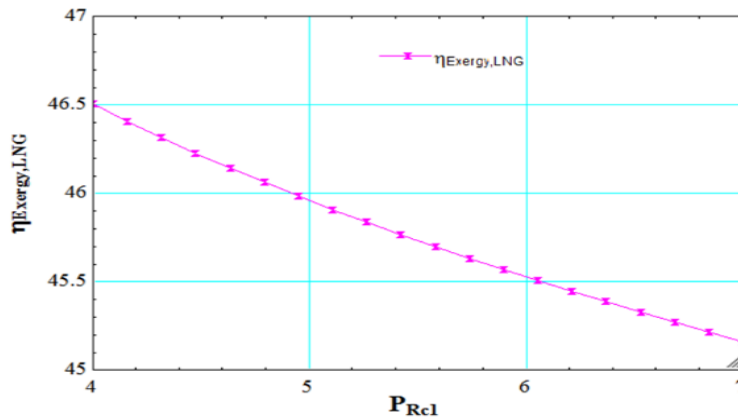


Figure 32. Variation of exergy efficiency of LNG-based cycle in terms of the compressor No.1 pressure ratio

According to Fig. 33, it is evident that by increasing the pressure ratio, the working generation of the cycle of increased primarily and then decreased. The reason can be explained that by increasing the pressure ratio, first, the generated work by turbine No.1 was increasing. On the other hand, the amount of consumed work by the compressor was also increasing. However, increasing the generated work by the turbine overcame the increase in the consumed work by the compressor and therefore increased the output power. In a range of

pressure ratios greater than 18, an increase in consumed work by the compressor overcame the increase in generated work by the turbine, which resulted in a decrease in net output power of the cycle.

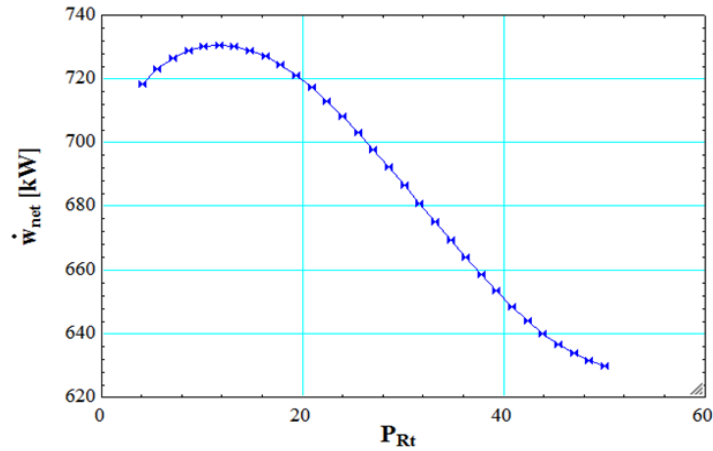


Figure 33. Variation of net power generation of LNG-based cycle in terms of the pressure ratio between 21 and 24 points

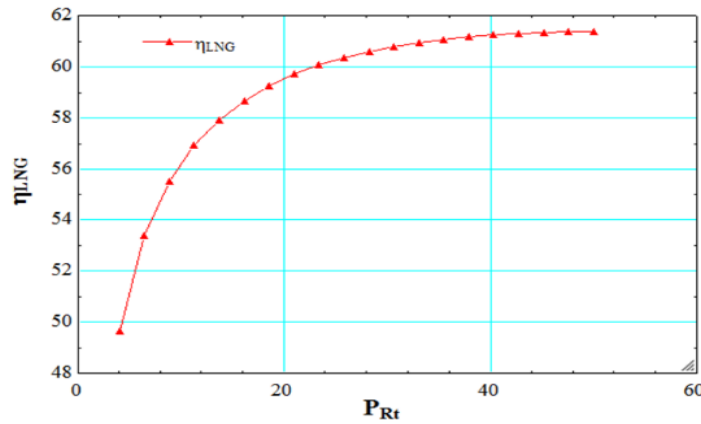


Figure 34. Variation of energy efficiency of LNG-based cycle in terms of the pressure ratio between 21 and 24 points

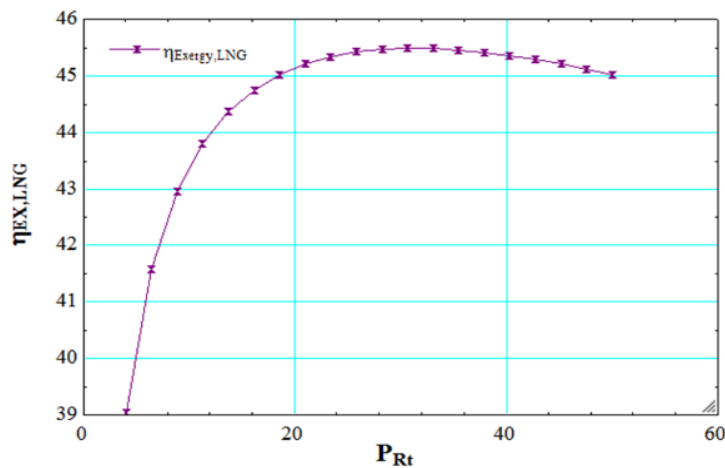


Figure 35. Variation of exergy efficiency of LNG-based cycle in terms of the pressure ratio between 21 and 24 points

According to Fig. 36, it is evident that by increasing the pressure ratio of Brighton mid-cycle with N2 fuel, the working generation of the cycle primarily increased and then decreased. The reason can be explained that by increasing the pressure ratio, the generated work by turbine No.2 was increasing at first. On the other hand, the amount of consumed work by the compressor was also increasing. However, increasing the generated work by the turbine overcame the increase consumed work by the compressor and therefore increases the output power. In a range of pressure ratios greater than 18, an increase in consumed work by the compressor overcame the increase in generated work by the turbine, which resulted in a decrease in the net output power of the cycle.

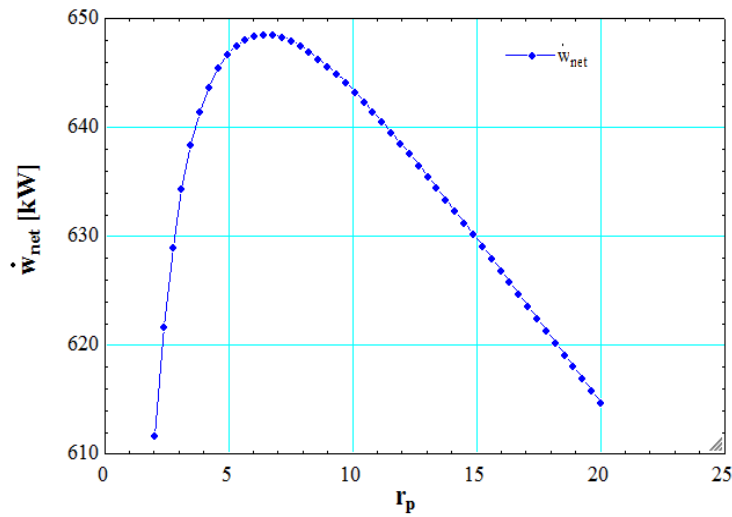


Figure 36. Variation of net power generation of LNG-based cycle in terms of the compressor pressure ratio in Brighton mid-cycle

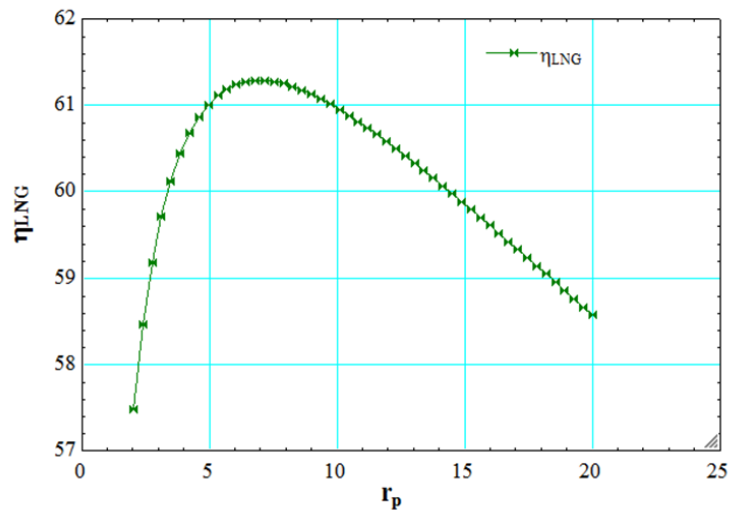


Figure 37. Variation of energy efficiency of LNG-based cycle in terms of the compressor pressure ratio in Brighton mid-cycle

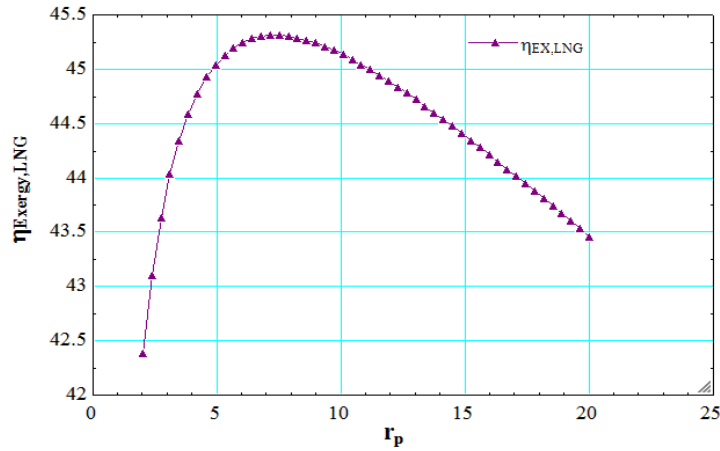


Figure 38. Variation of exergy efficiency of LNG-based cycle in terms of the compressor pressure ratio in Brighton mid-cycle

In order to review the performance of the cycle from the second law of thermodynamic perspective, the amount of exergy destruction for each component for the evaporator temperature was 5 ° C, the compressor No.1 pressure ratio of 6.575, and Brighton mid-cycle pressure ratio of 7 with N2 working fluid have been calculated and presented in Fig. 39.

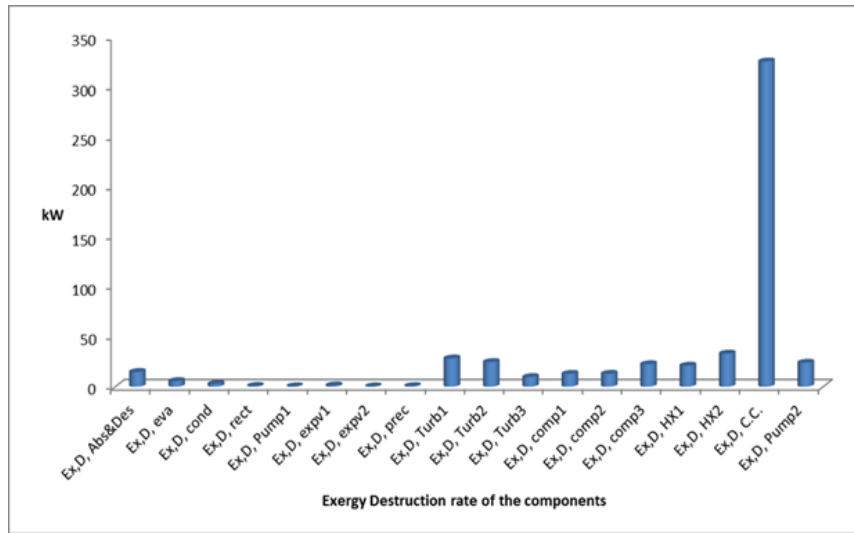


Figure 39. Comparison of exergy destruction in each component of the cycle for determined thermomechanical condition

Conclusion

An LNG-based CCP system and the energy recovery from the waste heat were proposed to be used in a GAX cycle and cooling generation. Modeling the cycle was carried out in EES Software. In order to ensure the precision of the obtained results of the LNG-based power generation system and the GAX cycle modeling, validation was carried out by comparing it with the results of the technical literature. The considered combined cycle was reviewed from the first and second laws of thermodynamics perspective. Furthermore, the evaluation of the some parameters was performed including the capacity of the refrigeration cycle, net generated power of the cycle, energy efficiency, exergy efficiency, and total exergy destruction, as well as the exergy destruction of each component of the cycle.

The overall and significant results obtained in the research were as follows:

1. According to the exergy analysis, the most exergy destruction occurred in the combustion chamber and heat exchanger No. 2, respectively.
2. The use of the GAX refrigeration cycle and the recovery of energy from the waste heat of the upstream cycle have been very effective in improving the overall cycle efficiency.

There is definitely a need for similar work and appropriate approaches to increase the efficiency of energy conversion systems from different perspectives. Therefore, the following suggestions were presented for future studies:

1. Use other refrigeration systems for energy recovery and evaluate the performance of the cycle.
2. It is suggested to investigate the combined cycle proposed in the present study from the economic perspective in order to determine the cost of refrigeration and power generation in the cycle and using evolutionary algorithms such as the genetic algorithm to determine the best operating point of the cycle.

Reference

1. Altenkirch E., Reversible absorptions maschinen XX, Jahrgang, Zeitschrift for die gesamteKalte-Industrie (1913) Heft 1:1e9, Heft 6:114e9.
2. Chiesa P. LNG receiving terminal associated with gas cycle power plants. ASME paper 97GT-441, 1997.
3. Desideri U, Belli C. Assessment of LNG vaporization system with cogeneration. ASME paper 2000-GT-0165, 2000.
4. Emmanuel C, Nicolas G, Martin D. Analysis of a carbon dioxide transcritical power cycle using a low temperature source. Appl Energy 2009;86:1055e63.
5. Foss MM. Introduction to LNG: an overview on liquefied natural gas (LNG), its properties, the LNG industry, safety considerations. Centre for Energy Economics, The University of Texas at Austin, www.beg.utexas.edu/energyecon/lng; 2003.
6. Garimella, S., Christensen, R.N., and Lacy D., 1996. Performance evaluation of a generator – absorber heat exchange heat pump, Applied Thermal Engineering. 16 (7): 591–406.
7. Greipentrog, H., & Sackarendt, P. (1976). Vaporization of LNG with closed cycle gas turbine. ASME paper 76-GT38, .6791
8. Hanawa K. An Ericsson GT design by LNG cryogenic heat utilization. ASME paper 2000-GT-166, 2000.
9. International energy outlook 2004, energy information administration. U.S. Department of Energy, www.eia.doe.gov/oiaf/ieo/elctricity.html; 2004.
10. Karashima N, Akutsu T. Development of LNG cryogenic power generation plant. In: Proceedings of 17th IECEC; 1982. p. 399–404.
11. Karellas S, Leontaritis AD, Panousis G, Bellos E, Kakaras E. Energetic and exergetic analysis of waste heat recovery systems in the cement industry. Energy 2013;58:147e56.
12. Gas, L. N. Current Expansion and Perspectives. 19-th Informatory Note on Refrigerating Technologies. International Institute of Refrigeration, Paris, France, November 2006.
13. Liu, M., Lior, N., Zhang, N., & Han, W. (2009). Thermoeconomic analysis of a novel zeroCO₂-emission high-efficiency power cycle using LNG coldness. Energy Conversion and Management, 50(11), 2768-2781.
14. Morosuk, T., & Tsatsaronis, G. (2011). Comparative evaluation of LNG-based cogeneration systems using advanced exergetic analysis. Energy, 36(6), 3771-3773.

15. Ng K.C., Tu K., Chua H.T., Gordon J.M., Kashiwagi T., Akisawas A., Thermodynamic analysis of absorption chillers, internal dissipation and process average temperature, *Appl. Therm. Eng.* 18 (8) (1998) 671e682.
16. Ramesh Kumar, A., and Udaya Kumar, M., 2008. Studies of compressor pressure ratio effect on GAX absorption compression cooler. *Applied Energy* 85(12): 1163–.27
17. Shi X, Che D. A combined power cycle utilizing low-temperature waste heat and LNG cold energy. *Energy Convers Manag* 2009;50:567e75.
18. Song Y, Wang J, Dai Y, Zhou E. Thermodynamic analysis of a transcritical CO₂ power cycle driven by solar energy with liquified natural gas as its heat sink. *Appl Energy* 2012;92:194e203.
19. Sugiyama, M., Ishida, M., Sasaki, T., & Ichimura, K. (1998). The operation technology of LNG terminals of Tokyo electric power company. In 12th LNG Utilization Conference.
20. Sun Z, Wang J, Dai Y. Exergy analysis and optimization of a hydrogen production process by a solar-liquefied natural gas hybrid driven transcritical CO₂. *Int J Hydrogen Energy* 2012;18731e9.
21. Szargut, J., & Szczygiel, I. (2009). Utilization of the cryogenic exergy of liquid natural gas (LNG) for the production of electricity. *Energy*, 34(7), 827-837.
22. Tsatsaronis, G., & Morosuk, T. (2010). Advanced exergetic analysis of a novel system for generating electricity and vaporizing liquefied natural gas. *Energy*, 35(2), 820-829.
23. Velautham S, Ito T, Takata Y. Zero-emission combined power cycle using LNG cold. *JSME Int J, Ser B. Fluids Therm Eng* 2001;44: 668–74.
24. Wang J, Wang J, Dai Y, Zhao P. Thermodynamic analysis and optimization of a transcritical CO₂ geothermal power generation system based on the cold energy utilization of LNG. *Appl Therm Eng* 2014;70:531e40.
25. Xue, X., Guo, C., Du, X., Yang, L., & Yang, Y. (2015). Thermodynamic analysis and optimization of a two-stage organic Rankine cycle for liquefied natural gas cryogenic exergy recovery. *Energy*, 83, 778-787.